

Investigation of Novel Quantum Dots/Proteins/Cellulose Bioconjugate Using NSOM and Fluorescence

Peng Zhang^{1,2}

Received October 13, 2005; accepted December 23, 2005
Published online: February 14, 2006

We investigated the engineered bioconjugate of cadmium selenide core/zinc sulfide shell, (CdSe)ZnS, quantum dots (QDs) with genetically modified proteins using fluorescence spectroscopy, near-field scanning optical microscopy (NSOM) and spectroscopy (NSOS). The protein polymer was allowed to self-assemble to the bacterial microcrystalline cellulose surface through the cellulosic binding domain. Results from the sample containing the QDs/protein/cellulose assemblies suggest that QDs were arrayed along the cellulose surface. The spectroscopic change of spectroscopic properties of the QDs upon bioconjugation, indicating the interaction among the immobilized QDs and between the constructed protein and QDs.

KEY WORDS: Fluorescence; near-field; spectroscopy; protein; quantum dots.

INTRODUCTION

The trend in device-oriented manufacturing toward smaller and smaller dimensions has fueled the need for nanofabrication techniques and a need for understanding the physics of nanometer-scale materials. The ability to understand and manipulate materials of such small dimensions has been facilitated by advances in surface imaging techniques, such as, STM, AFM, and the scanning transmission electron microscope (STEM).

Because of their physical size and the semiconductor material from which they are made, colloidal quantum dots (QDs) exhibit unique optical and electronic properties [1,2]. The study of semiconductor QDs systems has brought out many ideas in an effort to utilize the unique characteristics of QDs for specific applications. While the properties of isolated QDs offer a number of potential applications, their future use in electronic devices will require large arrays of QDs in a known order. Assembling these arrays in a known and controlled manner is

non-trivial. It requires the organization of mono-disperse quantum dots through a process that can be confirmed at the individual level [3,4].

To the other front, self-assembling of some natural proteins has been well understood. One method would be to use these proteins as templates for assembling nanomaterials, such as QDs, into simple structures and possibly arrays. Proteins can self-assemble, be similar to QDs in size, and be easily modified. One of the ideal systems for this application is the bacterial cellulosome protein complex, approximately 10–20 nm in diameter, because it can both self-assemble and respond to positional forces [5]. It is believed that cellulosome, a multi-protein complex produced by different cellulolytic microorganisms, can “collect” and “position” cellulose degrading enzymes onto a substrate [6]. The functional unit of the cellulosome, “scaffoldin,” contains repetitive domains of cohesins for specific interaction with other proteins containing a binding domain of dockerins. The cellulosome then self-assembles by specific cohesin/dockerin recognition. The scaffoldins can also contain surface binding domains, which act as a device to attach the cellulosome to the cell surface and/or substrate. By selecting the desired cohesin/dockerin pairs and positioning them in a proper order, all of the cellulosomal components

¹ Department of Chemistry, New Mexico Institute of Mining and Technology, Socorro, New Mexico 87801,

² To whom correspondence should be addressed. E-mail: pzhang@nmt.edu

(cohesins, dockerins, surface binding domains) can be cloned and expressed in *E. coli* [7] to produce engineered macromolecules [5]. These bioconjugates can then be immobilized onto cellulose surface through the surface binding domains. Essentially, the cellulose microfibrils would act as the templates for aligning the QDs into arrays.

Previously, there has been reported on the design and construction of a self-recognized protein polymer that can stabilize and assemble the (CdSe)ZnS QDs, as well as its characterization by STEM [8]. In this study, we report the application of fluorescence spectroscopy and near-field optical microscopy and spectroscopy to investigate the alignment of QDs onto the cellulose surface, as well as the interactions among the immobilized QDs.

EXPERIMENTAL

Cloning, expression, and purification of $6 \times$ histidine tagged CBM3 were as reported earlier [8]. In brief, PCR was applied to amplify the cohesin and dockerin genes from *C. thermocellum* genomic DNA. The two DNA fragments were purified, digested, and then ligated to form a new DNA fragment, which was then cloned and used to express the recombinant protein. Expressed proteins were purified before use. The apparent molecular weight of CBM3 was confirmed by SDS-PAGE.

Triethylphosphine/trioctylphosphine oxide (TOP/TOPO) passivated (CdSe)ZnS core-shell QDs were prepared using the reported procedures [1,2]. Excess TOP/TOPO were removed prior to use. The TOP/TOPO capping group was then replaced by mercaptopropionic acid (MPA) and titrated with Tris base to neutral pH [9].

For the near-field optical measurements, excess CBM3 protein was mixed with microcrystalline cellulose solution. The mixture was washed with buffer solution (0.020 M Tris pH 7.5, 0.001 M CaCl_2 and 0.100 M NaCl) three times to remove the protein complexes that are non-specifically bonded to the cellulose surface. The resulting protein/cellulose complexes were treated with solution containing MPA-Tris QDs. The mixture was again washed three times with Tris buffer to remove excess QDs. Lastly, a small amount of the final solution containing QD/CBM3/cellulose complex was spin cast onto a cover slip, and allowed to dry. For the steady-state optical measurements, $1 \mu\text{l}$ of MPA-Tris QDs solution was mixed with $50 \mu\text{l}$ of respective reactants, as described in the Results and Discussions section, for each run.

Near-field measurements were performed based on an Aurora-3 NSOM platform, equipped with a photo-

multiplier module, with a sensitivity of approximately 1 V/nW . The NSOM probe has an aperture diameter of approximately 100 nm. A 488 nm laser is used for all measurements. The laser power measured before coupling into the NSOM probe is approximately $250 \mu\text{W}$. Transmission signals are collected by an objective, passed through a super-notch holographic filter, and split by a beam splitter into the PMT, and a spectrometer equipped with a liquid nitrogen-cooled CCD detector and a single-photon APD attached to the two exit ports, respectively. This configuration allows various ways of collecting near-field signals. NSOM images can be generated through the PMT detector simultaneously with the topographical images. The NSOM probe can be moved to park above a spot of interest, and the CCD detector can generate a spectrum. Furthermore, the spectrometer can be set at a particular wavelength of interest, and the single-photon APD detector may generate an image at that specific wavelength with topographic image simultaneously. This system was successfully used for Raman study in the near-field of silver colloids [10].

The far-field steady-state fluorescence measurements are performed on a home-built confocal setup using the same spectrometer/CCD detector as in the NSOM experiments. A droplet of solution was placed on a cover slip above a $40 \times$ objective. The laser beam was focused by this objective onto the droplet. The emitting signals were collected by the same objective, reflected by a beamsplitter and then focused onto the same fiber used in the Aurora-3 system that is connected to the spectrometer.

RESULTS AND DISCUSSIONS

All images in Fig. 1 are collected simultaneously. Topographic image of the QD/protein/cellulose film is generated by the NSOM probe, and shown in Fig. 1a. Figure 1b is the optical image generated by the PMT detector. This image is composed predominantly of the QDs fluorescence, as the majority of Rayleigh scattering has been filtered out by the super-notch filter. Figure 1c is the image generated by the avalanche photon detector (APD), with the spectrometer set at the peak of the quantum dots fluorescence. This image is thus solely composed of the quantum dots fluorescence signal at 530 nm. The excitation intensity at the tip of the NSOM probe is at most a few nanowatts, resulting in an extremely weak fluorescence signal. During the scanning, the NSOM probe stopped at each pixel for 300 ms to allow the APD to integrate the fluorescence signal.

The tube-like object in the topographic image, Fig. 1a, is a portion of a cellulose microfibril. The

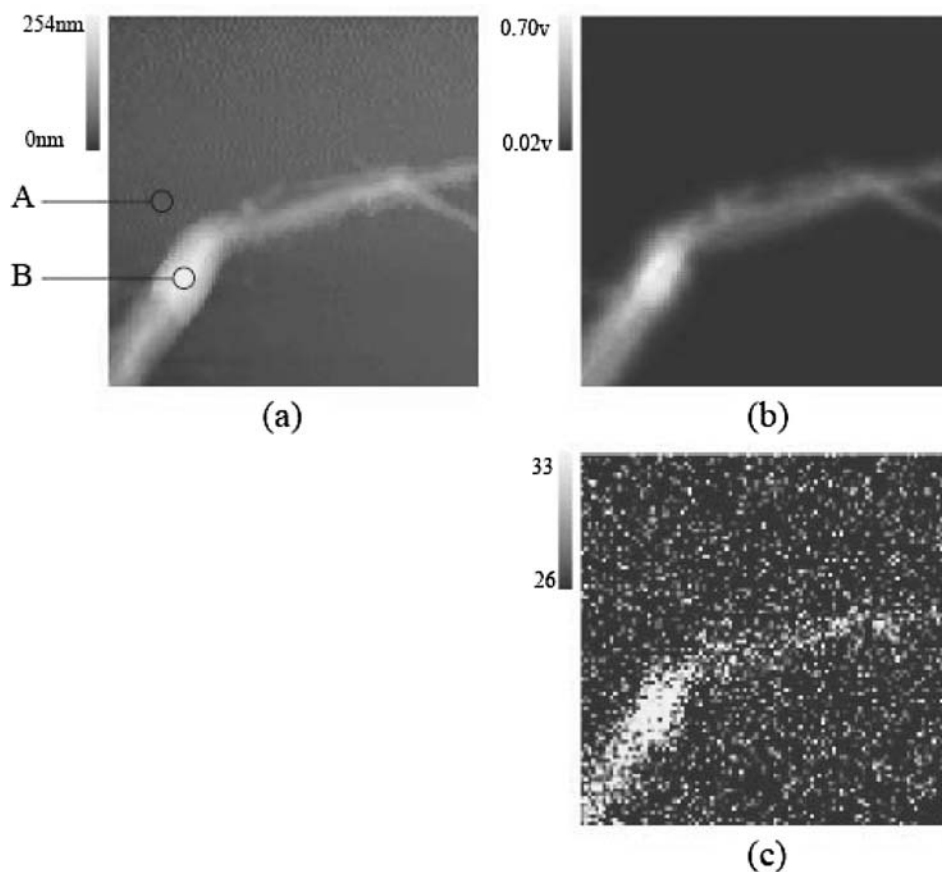


Fig. 1. Topographic image (a), NSOM image (b), and near-field fluorescence ($\lambda = 530 \text{ nm}$) (c) of a $5 \mu\text{m} \times 5 \mu\text{m}$ portion of a sample of QD/CBM3/cellulose complex.

NSOM image, Fig. 1b, displays good correlation with the topographic image, indicating that QDs are aligned along the cellulose surface as designed. The near-field fluorescence image, Fig. 1c, further confirms that the NSOM image is not due to artifacts. In addition, after the imaging we parked the NSOM probe above two spots (A, B) within the area shown in Fig. 1a and collect the fluorescence spectra, as shown in Fig. 2. While spot A has little fluorescence signal of QDs, spot B shows an obvious fluorescence peak. This observation directly validates the scheme of using cellulose as template for aligning QDs. It also demonstrates the effectiveness of the bioengineered cohesin/docker protein (CBM3).

To further understand the interaction between QDs and CBM3, steady-state fluorescence measurements were taken for the following mixtures: QDs only in buffer (1), QDs mixed with bovine serum albumin (BSA, a general protein) (2), QDs mixed with CBM3 (3), and QDs/CBM3/cellulose complex (4). QDs concentrations

($1 \mu\text{M}$) were kept constant in all runs. The results are shown in Fig. 3, with the intensity normalized according to the incident laser intensity. Notice that the addition of BSA does not seem to affect the fluorescence intensity and peak position much, implying there is little interaction between QDs and BSA. The slight increase in fluorescence intensity for (2) is probably due to the fact that addition of BSA increases the scattering of the solution.

The scenario is quite different for the other two mixtures, (3) and (4). First, both QDs/CBM3 mixture and QDs/CBM3/cellulose mixture exhibit significantly higher fluorescence intensity. Also, both fluorescence peaks are red-shifted, by approximately 7 and 12 nm, respectively. We suggest that the dramatic increase in fluorescence intensity could be due to the strong interaction between QDs and CBM3 protein, which effectively makes the QDs much “heavier” and thus stay longer in the focused zone. The fluorescence red shift also indicates the existence of this interaction. The chemistry of Zn-histidine coordination is well understood and has been widely used

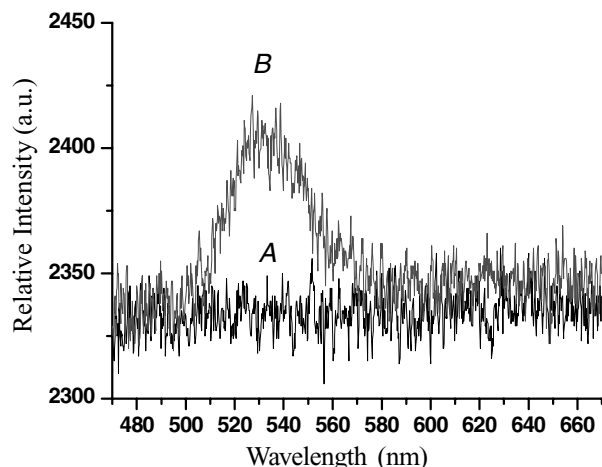


Fig. 2. Near-field fluorescence spectra taken at two spots A and B, as shown in Fig. 1a. Integration time is 300 s.

for the purification of tagged proteins and more recently applied to QD bioconjugation [11]. We suggest that the Zn-histidine coordination lead to the lowering of the QDs band gap, thus the fluorescence red-shift.

It is worthwhile to further compare (3) and (4). In both cases, the QDs are bound to the $6 \times$ histidine tagged CBM3. There is no direct contact between the QDs and the cellulose. Thus, it is intriguing to observe the further fluorescence red shift for QDs/CBM3/cellulose as compared to QDs/CBM3. Besides, one would expect fluorescence intensity for (4) to be higher than that for (3), as the QDs/CBM3/cellulose complex is obviously much heavier than the QDs/CBM3 complex. The fact that the opposite

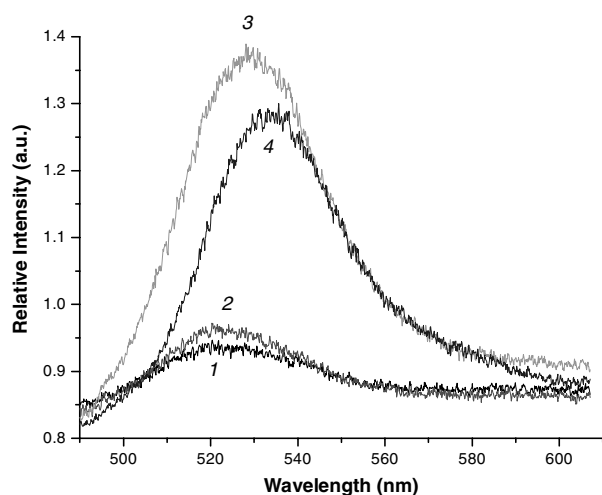


Fig. 3. Steady-state fluorescence spectra of four mixtures containing same amount of QDs: 1, QDs/buffer; 2, QDs/BSA; 3, QDs/CBM3; 4, QDs/CBM3/cellulose.

is observed suggests other mechanisms may be in effect. We argue that one possible explanation to these observations is that there may be energy transfer (communication) taking place between QDs after their alignment onto the cellulose surface, a subject for further investigations.

In conclusion, we report the investigation of the (CdSe)ZnS QDs/recombinant proteins/cellulose complex using NSOM and steady-state fluorescence measurements. A genetically engineered protein polymer was expressed, purified, and allowed to self-assemble to the bacterial cellulose surface. QDs were then conjugated to the protein/cellulose assembly. Near-field optical microscopic observations confirm that QDs are arrayed along the cellulose surface. The fluorescence results demonstrate the strong interaction between recombinant protein and the QDs. They also indicate the possible communication between immobilized QDs after they are bound into arrays. These results are complement to the recent STEM study on the same type of assembly [8]. They support the notion that inorganic/biological conjugates have promise in designing and fabricating devices at the nanometer scale.

ACKNOWLEDGMENTS

The author sincerely acknowledges Drs. Mike Himmel and Shiyong Ding, both of National Renewable Energy Laboratory, Golden, CO, for the access of facilities and the help of sample preparations.

REFERENCES

1. M. G. Bawendi, P. J. Carroll, W. L. Wilson, and L. E. Brus (1992). Luminescence properties of CdSe quantum crystallites—Resonance between interior and surface localized states. *J. Chem. Phys.* **96**, 946–954.
2. Z. A. Peng and X. G. Peng (2001). Formation of high-quality CdTe, CdSe, and CdS nanocrystals using CdO as precursor. *J. Am. Chem. Soc.* **123**, 183–184.
3. C. R. Kagan, C. B. Murray, M. Nirmal, and M. G. Bawendi (1996). Electronic energy transfer in CdSe quantum dot solids. *Phys. Rev. Lett.* **76**, 1517–1520.
4. O. I. Micic, S. P. Ahrenkiel, and A. J. Nozik (2001). Synthesis of extremely small InP quantum dots and electronic coupling in their disordered solid films. *Appl. Phys. Lett.* **78**, 4022–4024.
5. S.-Y. Ding, R. Lamed, E. A. Bayer, and M. E. Himmel (2003). In: J. Setlow (Ed.), *Genetic Engineering: Principles and Methods*, Vol. 25. Kluwer Academic, New York, p. 209.
6. E. A. Bayer, E. Morag, and R. Lamed (1994). The cellulosome—A treasure-trove for biotechnology. *Trends Biotechnol.* **12**, 379–386.
7. S.-Y. Ding, M. T. Rincon, R. Lamed, J. C. Martin, S. I. McCrae, V. Aurilia, Y. Shoham, E. A. Bayer, and H. J. Flint (2001). Cellulosomal scaffoldin-like proteins from *Ruminococcus flavefaciens*. *J. Bacteriol.* **183**, 1945–1953.
8. S.-Y. Ding, G. Rumbles, M. Jones, M. P. Tucker, J. M. Nedeljkovic, M. N. Simon, J. Wall, and M. E. Himmel (2004). Bioconjugation of (CdSe)ZnS quantum dots using a genetically engineered multiple

- polyhistidine tagged cohesin/dockerin protein polymer, *Macromol. Mater. Eng.* **289**, 622–628.
9. S.-Y. Ding, M., Jones, M. P., Tucker, J. M., Nedeljkovic, J., Wall, M. N., Simon, G., Rumbles, and M. E., Himmel (2003). Quantum dot molecules assembled with genetically engineered proteins, *Nano Lett.* **3**, 1581–1585.
 10. P. Zhang, S. Smith, G. Rumble, and M. Himmel (2005). Direct imaging of surface-enhanced Raman scattering in the near field, *Langmuir* **21**, 520–523.
 11. I. L. Medintz, A. R. Clapp, H. Mattoussi, E. R. Goldman, B. Fisher, and J. M. Mauro (2003). Self-assembled nanoscale biosensors based on quantum dot FRET donors, *Nature Mater.* **2**, 630–638.